Coupled Expression and Colocalization of 140K Cell Adhesion Molecules, Fibronectin, and Laminin during Morphogenesis and Cytodifferentiation of Chick Lung Cells

Wen-Tien Chen, Jinq-May Chen, and Susette C. Mueller

Department of Anatomy and Cell Biology, Georgetown University Medical Center, Washington, D.C. 20007

Abstract. We have analyzed the expression and distribution of fibronectin, laminin, and the 140K cell adhesion molecules (140K complex) in embryonic chick lung cells by a combination of biochemical and immunofluorescent approaches. The 140K complex was identified by monoclonal antibody JG22E as a complex of glycoproteins averaging 140,000 M_r and has been implicated in vitro as a receptor for fibronectin and laminin. Our studies provide the first description that the 140K complex is developmentally regulated, and that the 140K complex appears to be involved in adhesion of epithelial and endothelial cells during morphogenesis. We have shown that the 140K complex is expressed in high quantity in embryonic lung cell types, but is markedly reduced in all of the differentiated cell types except smooth muscle. Embryonic lung cells are enriched in 140K complex on portions of cells in close proximity to areas rich in fibronectin. For example, during the formation of airways and alveolar tissues, 140K complex is concentrated at the basal surfaces of epithelial cells adjacent to fibronec-

tin. Likewise, during the angiogenic invasion of capillaries into lung mesenchyme, the 140K complex becomes localized at sites on the basal surfaces of endothelial cells in close contact with fibronectin. Finally, cytodifferentiating lung smooth muscle cells show unusually high levels of 140K complex, fibronectin, and laminin that persist into the adult. In contrast to fibronectin, laminin is found to be uniformly distributed in the basement membranes of differentiating epithelial cells. It becomes prominent in adult alveolar epithelium and airway epithelium concomitant with a reduction or loss of 140K complex and fibronectin at cell–basement membrane attachment sites. Surprisingly, laminin is also present in a punctate pattern in the mesenchyme of early lung buds, however, laminin, fibronectin, and 140K complex are greatly reduced or lost during mesenchymal maturation. Our results are consistent with the active participation of the 140K complex in cell-to-matrix adhesion during morphogenesis of alveolar walls and cytodifferentiation of mesenchymal and smooth muscle cells.

A DHESIVE interactions of cells with the extracellular matrix (ECM)[1] are critically important events for morphogenetic movements and cytodifferentiation during embryonic development and for the maintenance of tissue structure and function (45, 47). These processes could be guided by temporal and spatial changes in the composition of cell adhesion molecules (20) in the cell membrane that interact with other cells or with ECM molecules such as fibronectin and laminin. Although modulation of specific classes of cell adhesion molecules might play an important regulative role in morphogenesis by linking cells together (13, 14, 20, 39), it is not known whether there are specific cell adhesion molecules that react with ECM components to shape developmental events.

Cell–matrix interactions occur at discrete membrane regions in cultured cells and appear to be mediated by integral membrane receptors for fibronectin (1, 3, 4, 6, 11, 12, 18, 25, 27, 28, 31, 32, 38, 40) and laminin (28, 34, 35, 36). In several types of avian cells, a complex of glycoproteins, averaging 140,000 in apparent molecular mass on SDS polyacrylamide gels (referred to here as the 140K complex) appears to be involved in the binding of cells to fibronectin (1, 3, 11, 12, 17, 18, 19, 25, 27, 28, 31, 38). The evidence supporting this includes immunological inhibition studies (3, 4, 11, 17, 18, 19, 25, 38) and direct binding of such molecules to fibronectin (1, 28, 40). In earlier in situ localization studies using immunolabeling of frozen-thin sections (FTS), we demonstrated the 140K complex distribution at attachment sites of the plasma membrane in cultured fibroblasts, and in smooth muscle and epithelium (7, 12, 19, 43). In double- and triple-labeling experiments, the 140K complex colocalizes with

---

1. *Abbreviations used in this paper:* DIC, Nomarski differential interference contrast microscopy; ECM, extracellular matrix; FTS, frozen-thin sections.

both fibronectin and microfilament bundles, which suggests that the 140K complex may be part of a cell surface linkage between fibronectin and the cytoskeleton (11, 17). Whereas some structural aspects and the membrane localization of the 140K complex have been investigated, its contributions to cell–matrix interactions during embryogenesis have remained elusive, particularly in epithelia and endothelia.

A fundamental question raised by observations of morphogenetic movements and cytodifferentiation is: how do cells attach to the ECM and later detach to translocate (45)? The role of fibronectin in linking cells and other ECM molecules in lung tissue organization and repair has been proposed (24, 37, 42, 44). On the basis of previous studies on fibronectin-mediated adhesion in myoblasts, fibroblasts, and neural crest cells (for examples, see references 3, 11, 12, 19, and 22), it has been proposed that the 140K complex interacts with fibronectin to provide the labile, motility-related cell adhesion necessary for morphogenetic movements. If this is so then these molecules should be expressed at distinct sites on the cell surface and undergo modulation in quantity or position during expression of specialized cell functions. The only evidence, to date, that the 140K complex plays an important role in morphogenesis comes from antibody inhibition studies on neural crest cell migration that involves fibronectin-mediated adhesion (3, 19). In contrast, laminin and 140K complex have been localized to epithelial cells (12, 21, 23, 30), but their associations during differentiation of epithelial and endothelial cells have not been investigated.

In this study, we examined the amount and distribution of 140K complex, fibronectin, and laminin during functional development of chick embryonic lungs. To form the complex alveolar tissues, lung epithelial cells and capillary endothelial cells participate in active morphogenetic movements, and mesenchymal fibroblasts and smooth muscle cells undergo cytodifferentiation. Our aims were to relate the coupled expression of 140K complex and fibronectin or laminin at discrete sites on the cell surface to: (a) differentiation of functional epithelial cells (particularly the formation of fibronectin- and laminin-positive basement membranes); (b) angiogenic invasion of capillary endothelial cells; (c) mesen-

chymal maturation; and (d) to smooth muscle differentiation. The lung is a very useful model system to study the function of the 140K complex because it contains multiple cell types that, during adhesion-mediated developmental events, interact with ECM.

To obtain in vivo evidence relating subcellular structures to protein localization in embryonic lungs, we used a combination of biochemical analysis, double immunofluorescent labeling, and frozen-thin sectioning. We have found that the 140K complex is developmentally regulated, it is prominently expressed in all differentiating lung cell types, and it colocalizes with fibronectin at cell–matrix adhesion sites during lung development. Our results are consistent with the proposal that the 140K complex plays an active role in cell-to-matrix adhesion in epithelial and endothelial cells during morphogenesis of alveolar walls and in mesenchymal and smooth muscle cells during cytodifferentiation.

Materials and Methods

Chicken Embryos

White leghorn chick embryos (Truslow Farms Inc., Chestertown, MD) were used throughout the study. Eggs were incubated at 38 ± 1°C in a humidified air chamber and staged according to Hamburger and Hamilton (26) and the duration of incubation.

Frozen-thin Sectioning of Lungs

Fresh tissue, dissected out of the middle part of the lower lobe of the lung, was cut into 1-mm^3 cubes in the presence of 3% paraformaldehyde in PBS (0.13 M NaCl in 0.02 M sodium phosphate buffer [pH 7.4]) plus 0.5 mM MgCl$_2$, 0.5 mM CaCl$_2$, and 60 mM sucrose. The tissue was then fixed for 30 min at room temperature and infused with 0.3% paraformaldehyde and 0.6 M sucrose in PBS at 4°C overnight. The fixed tissue blocks were mounted on a copper specimen holder and frozen in liquid nitrogen. 0.5-μm frozen-thin sections (FTS) were cut at −40°C using a glass knife according to the methods described previously (12). The sectioning was performed with an ultramicrotome (model MT-2B; E. I. DuPont de Nemours & Co., Inc., Sorvall Instruments Div., Newton, CT) with a cryoattachment. FTS were transferred by means of a small wire loop containing a droplet of 2.3 M sucrose onto a glass slide for immunofluorescent labeling and light microscopic observations.

Table I. Relative Abundance of Embryonic Chick Lung Epithelial, Endothelial, and Mesenchymal Cells during Egg Incubation

Incubation*	Cell number (10³/mm²)‡			
	Epithelium	Endothelium	Mesenchyme	Total
d				
Glandular				
5	2.4 ± 0.5 (17)	0	11.7 ± 1.1 (83)	14.1
9	4.1 ± 0.7 (37)	0	7.1 ± 1.1 (63)	11.2
Vascular				
13	8.6 ± 1.0 (65)	1.2 ± 0.2 (9)	3.4 ± 0.6 (26)	13.2
Alveolar				
18	11.0 ± 2.2 (61)	4.2 ± 1.0 (24)	2.7 ± 0.1 (15)	17.9
Hatched	5.9 ± 0.1 (52)	4.0 ± 0.5 (35)	1.5 ± 0.4 (13)	11.4

* Lung size was determined to be 5 mg for 5 d, 20 mg for 9 d, 136 mg for 13 d, 208 mg for 18 d, and 401 mg for hatched chick lung; these lung weights were measured by averaging the weight of 46 lung buds for 5 d stage, 34 lungs for 9 d, 23 lungs for 13 d, 11 lungs for 18 d, and six lungs for hatched chicks.
‡ Relative numbers were obtained by counting cells of randomly chosen, developing alveolar regions within an 100 × 100-μm² area of 0.5 μm FTS. For a given section, the total cell number in 10 separate 100 × 100-μm² areas was taken as one determinant. The developing airway regions containing smooth muscle adjacent to parabronchi usually occupy ∼15% of total section areas of lungs at different developmental stages and were not included. Means and standard deviations were calculated from six determinations of independent sections taken from two different lungs. Numbers in parentheses indicate percent of total cells in the developing alveolar regions.

Immunolabeling Reagents

JG22E mouse monoclonal antibody directed against the complex of 140K glycoproteins (140K complex) and rabbit polyclonal anti-140K complex antibodies were prepared and characterized as described (11). Rabbit polyclonal anti-fibronectin antibodies (9, 11) and anti-laminin antibodies (and guinea pig anti-laminin antibodies, both gifts from Dr. Charles Little, University of Virginia at Charlottesville, VA) were affinity purified on the relevant antigen coupled to Ultrogel AcA-22 (LKB Instruments, Inc., Gaithersburg, MD) and their specificity was demonstrated by an enzyme-linked immunosorbent assay and an immunoblot assay using purified fibronectin or laminin. Rhodamine-conjugated goat antibodies to mouse IgG and fluorescein-conjugated goat antibodies to rabbit IgG (or to guinea pig IgG) were immunoaffinity-purified and cross-adsorbed as described (10).

Indirect Immunofluorescent Labeling of FTS

FTS of tissues attached to glass slides were indirectly double-immunolabeled according to the following two-stage labeling procedure: (a) immersion in PBS for 5 min to remove the 2.3 M sucrose used for transferring the sections; (b) reaction of free aldehyde groups with 0.1 M glycine and blocking of nonspecific binding sites with 1% gelatin in PBS; (c) incubation in a mixture of primary antibodies consisting of JG22E mouse monoclonal IgG and rabbit anti-fibronectin or rabbit anti-laminin IgG (or guinea pig anti-laminin and rabbit anti-fibronectin polyclonal antibodies), each at a concentration of 10 μg/ml for 10 min; (d) after three rinses in PBS, incubation in a mixture of two cross-adsorbed secondary antibody conjugates (fluorescein-goat anti-rabbit IgG and rhodamine-goat anti-mouse IgG, or fluorescein-goat anti-rabbit IgG and rhodamine-goat anti-guinea pig IgG) each at a concentration of 20 μg/ml for another 10 min; and (e) rinsing in PBS and mounting in 90% glycerol and 10% Tris-HCl buffered at pH 8. This two-stage double-labeling method produced strong labeling and allowed us to photograph the fluorescent image within 30 s of exposure to mercury illumination. Control experiments for double-labeling were performed as previously described (11).

Immunofluorescently labeled FTS were observed with a Zeiss Photomicroscope III fitted with vertical illuminator RS III for epifluorescence
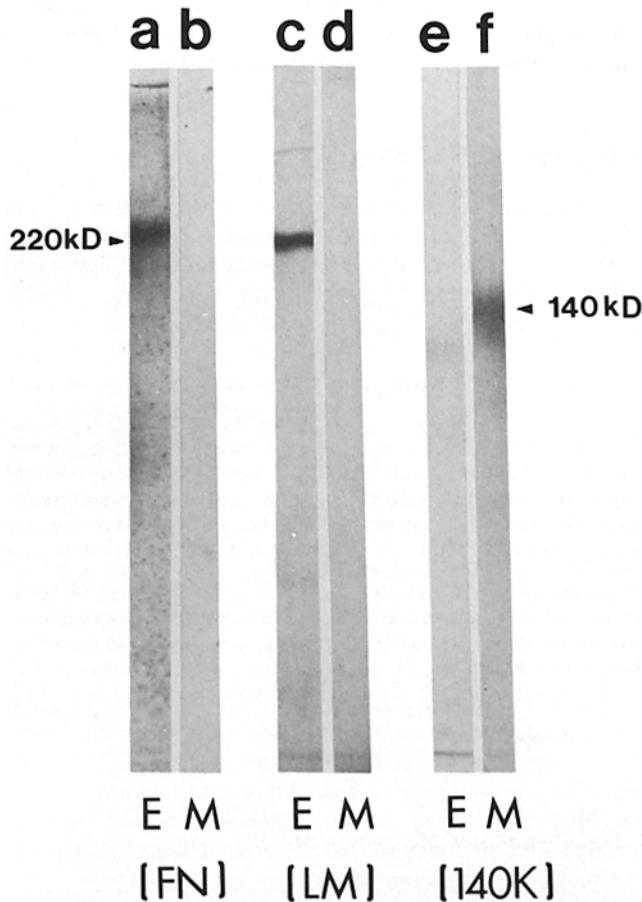

Figure 1. Western immunoblot analysis of fibronectin (FN), laminin (LM), and 140K complex (140K) from membrane extracts (M) and ECM extracts (E) of embryonic chick lungs at 18-d incubation. The ECM was extracted from chick lungs with 50 mM Tris-HCl buffer (pH 7.5), containing 0.5 M NaCl, 1 M urea, 2 mM N-ethylmaleimide, and 1 mM phenylmethylsulfonyl fluoride. The residue was further extracted with 1% Triton X-100 in 10 mM Tris-HCl (pH 7.5) containing 0.5 mM CaCl₂, 2 mM N-ethylmaleimide, and 1 mM phenylmethylsulfonyl fluoride. The detergent-soluble fraction was designated the membrane extract (see Materials and Methods). Extracts were solubilized in SDS under reducing conditions, separated by 6% SDS PAGE, electrophoretically transferred to nitrocellulose, and labeled with specific rabbit polyclonal antibodies (see Materials and Methods for detailed immunoblot procedure and characterization of antibodies). In all samples examined, fibronectin was reduced to monomers that migrated at 220 kD. Most laminin was also reduced to 220-kD monomers, but a small amount of laminin appeared to remain as dimers, shown as a faint 440-kD band.
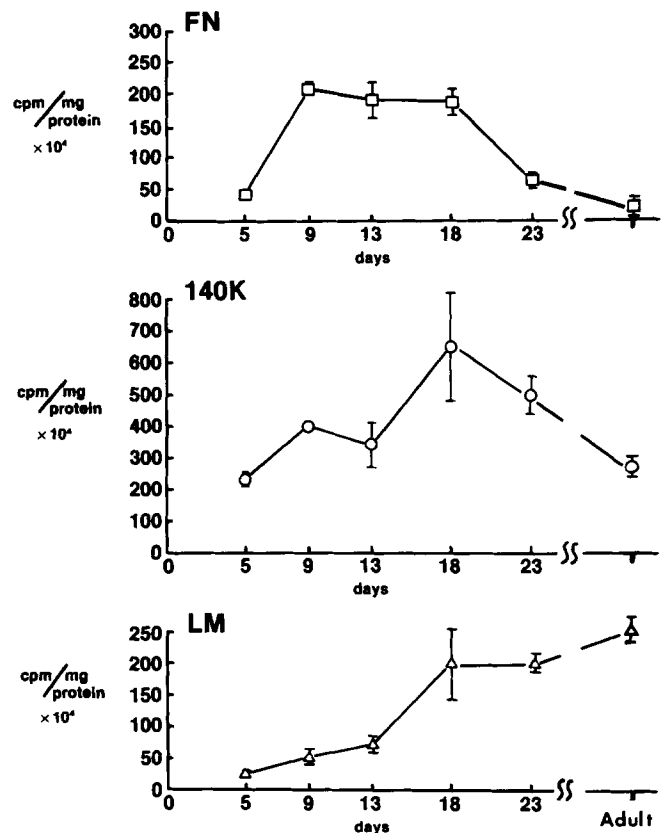

Figure 2. Quantitation of fibronectin (FN), 140K complex (140K), and laminin (LM) present in chicken embryonic lungs at various stages of development using rabbit anti-fibronectin, rabbit anti-laminin, and rabbit anti-140K complex antibodies and dot immunoblot analysis (see Materials and Methods). The amount of 140K complex (per milligram protein in lung membrane extracts) was greatest in embryonic lungs at the vascular stage compared with lungs in other stages of development. Fibronectin was highest in concentration in ECM extracts from lungs at the glandular stage, but was reduced in concentration in lungs at the alveolar stage as well as in adult lungs. Laminin increased in concentration throughout development. In adult chicken lungs, both 140K complex and fibronectin were found in significantly lower amounts (fivefold less) compared with embryonic lungs at the vascular stage, but laminin levels remained high after the alveolar stage.

and with transmitted light for Nomarski differential interference contrast (DIC) and phase-contrast images. A Plan-Neofluar 25/0.8 phase objective (Carl Zeiss, Inc., Thornwood, NY) was used for routine observations of tissue sections and a Planapo 63/1.4 objective (Carl Zeiss, Inc.) for high resolution studies on single cells in the sections.

Quantitative Immunofluorescence

Measurements of relative fluorescence intensity on individual lung cells were performed by using the spot measurement on the Zeiss Photomicroscope III. Using the Planapo 63/1.4 objective, specific areas of cells or structures on lung sections (for example, apical and lateral vs. basal surfaces of columnar epithelial cells, mesenchymal fibroblasts vs. smooth muscle cells, etc.) were placed in the circle in the center of the reticle field. Measurements were made by closing the field diaphragm to 3 µm in diameter, setting the automatic exposure at ASA 6400, and recording the time in seconds required to reach 50% exposure. Measurements were expressed in arbitrary units by defining the intensity of anti-140K complex staining on the lateral surface of columnar lung epithelial cells as one unit, and the fibronectin (or laminin) staining on the mesenchyme as one unit. In the same FTS, this fluorescence quantitation is highly reproducible. When the same labeled structures on different FTS are compared, variability increases slightly primarily due to differences in section thickness.

Dot Immunoblot and Western Immunoblot Analyses

Fibronectin and laminin were extracted from chick lungs with 50 mM Tris-HCl buffer (pH 7.5) containing 0.5 M NaCl, 1 M urea, 2 mM N-ethylmaleimide and 1 mM phenylmethylsulfonyl fluoride (Sigma Chemical Co., St. Louis, MO) by first homogenizing and then stirring overnight at 4°C. The extract was cleared by centrifugation at 100,000 g for 1 h and designated the ECM extract. The residue was then extracted with 1% Triton X-100 in 10 mM Tris-HCl buffer (pH 7.5) containing 0.5 mM CaCl₂, 2 mM N-ethylmaleimide and 1 mM phenylmethylsulfonyl fluoride, and the detergent-soluble fraction was designated the membrane extract. Proteins were measured by assaying the extracts with the Bio-Rad protein assay (Bio-Rad Laboratories, Richmond, CA) using BSA as standard.

20 µg of protein from either the membrane or ECM extract was resolved under reducing conditions by 6% SDS PAGE and then Western immunoblotting was performed as described (5) using transfer buffer without SDS (11). Immunoreactivity of anti-140K complex, anti-fibronectin, and anti-laminin antibodies with polypeptides from the membrane or ECM extracts from lung was visualized by incubating the blots with horseradish peroxidase-antibody conjugates followed by development in 0.05% diaminobenzidine, 50 mM Tris-HCl (pH 7.4) and 0.03% H₂O₂.

To quantitate 140K complex from lung, 10 µl of the membrane extract (containing ~20 µg of protein) was spotted within a circle (0.5 cm in diameter) on nitrocellulose membrane filters (pore size, 0.22 µm; Schleicher & Schuell, Keene, NH) and dot immunoblot analysis was performed as described (29) using purified 140K complex (obtained from JG22E-immunoaffinity chromatography) as standards. Fibronectin and laminin from ECM extracts of lungs were quantitated in the same way using affinity-purified antibodies, either rabbit anti-fibronectin or rabbit anti-laminin, and purified chicken cellular fibronectin and mouse Englebreth-Holm swarm tumor laminin as standards.

Results

### Morphology and Cytodifferentiation of Embryonic Chick Lungs

The development of chick lung proper can be divided into three embryonic periods: the glandular period (3-12 d of egg incubation), the vascular period (12-16 d of incubation), and the alveolar period (from 16 d to hatching), culminating in the eventual formation of air-blood barriers. (For a detailed description of the terminology and of chick lung morphogenesis, see references 2, 15, 16, and 26).

Except for the peculiar formation of bronchial circuits and large nonrespiratory air sacs in birds, the histological events occurring during the three periods of chick lung formation are similar to those occurring during the three periods of mammalian lung development (2). In chicks, the glandular period is characterized by the active division of cells in the central epithelial tubules, which are embedded within a large mass of undifferentiated mesenchyme (see Figs. 3 and 4). The tertiary bronchi or parabronchi have started to branch out and grow towards each other to form the airway. Also during this period, on day 9, clusters of smooth muscle cells appear in the mesenchyme adjacent to the outpocketing parabronchi (see Fig. 4, 9d). The vascular period occurs between 12 and 16 d of incubation and is analogous to the canalicular stage in mammalian lung (from 19-20 d in the fetal rat; reference 2). The atrium buds off from the parabronchial epithelium, the mesenchyme condenses, and a network of capillaries invades the mesenchyme next to the atrium. Epithelial cells change their shape from columnar to squamous in the developing airway during the vascular period, whereas in developing alveoli the epithelial cells undergo this shape change later, during the early alveolar period. Smooth muscle cells grow into crisscross bundles that line the openings of atria and parabronchi (see Figs. 7 B, and 8, A and B). In the developing alveolar walls, mesenchymal condensation and extensive vascularization continue until the alveolar period. Eventually the basement membrane of capillary endothelia fuses with that of the alveolar epithelia to form the air-blood barriers (see Figs. 7 B, and 8, A and B). In the days that remain before hatching, the walls of the airways, including atria and parabronchi, become covered with smooth muscle bundles and with a network of arterioles and veinules of the pulmonary vascular system. Air is first taken into the chick lungs 1 or 2 d before hatching (the 19th day of egg incubation), when the chick bill enters the air chamber. At this time the arterial ducts begin to contract, forcing an increased flow of blood into the lungs. After hatching, the alveolar walls continue to grow and more air is taken into the lungs so that the expanded alveoli become the major lung structure facilitating gas exchange.

During lung development, the relative number of mesenchymal cells decreases, while developing alveolar epithelial cells and capillary endothelial cells increase in number and extend towards each other to form the alveolar walls. Table I shows the relative abundance of epithelial, endothelial, and mesenchymal cells in chick lungs at different embryonic stages. These numbers were derived by counting cells in 0.5 µm FTS of lung tissue. Epithelial cells increase in rela-

Figure 3. In situ immunofluorescent distribution of 140K complex (*140K*), fibronectin (*FN*), and laminin (*LM*) on FTS of chicken embryonic lungs at the glandular stage (5 d). (*A*) Cross section of a lung bud seen with phase-contrast microscopy and double-labeled for 140K complex (monoclonal JG22E) and FN (monospecific rabbit anti-FN). The 140K complex is concentrated at the phase-dark, basal surfaces of both columnar epithelial cells (*arrows*) and cuboidal mesothelial cells (*open arrows*), as well as on the cell surface of mesenchymal cells; these 140K complex-positive structures are also labeled for fibronectin. The apical and lateral surfaces of epithelial and mesothelial cells are more weakly labeled with anti-140K complex and not labeled at all with anti-fibronectin. (*B* and *C*) Mesothelial lining cells (*B*) and epithelial cells (*C*) of a lung bud are double-labeled for LM (monospecific guinea pig anti-LM) and FN. LM is found not only in the usual basement membrane localization, but also on the mesenchymal cells. FN is less intensively labeled throughout the LM-positive regions. Note that in the mesenchyme, FN and LM staining do not coincide. Bar, 20 µm.
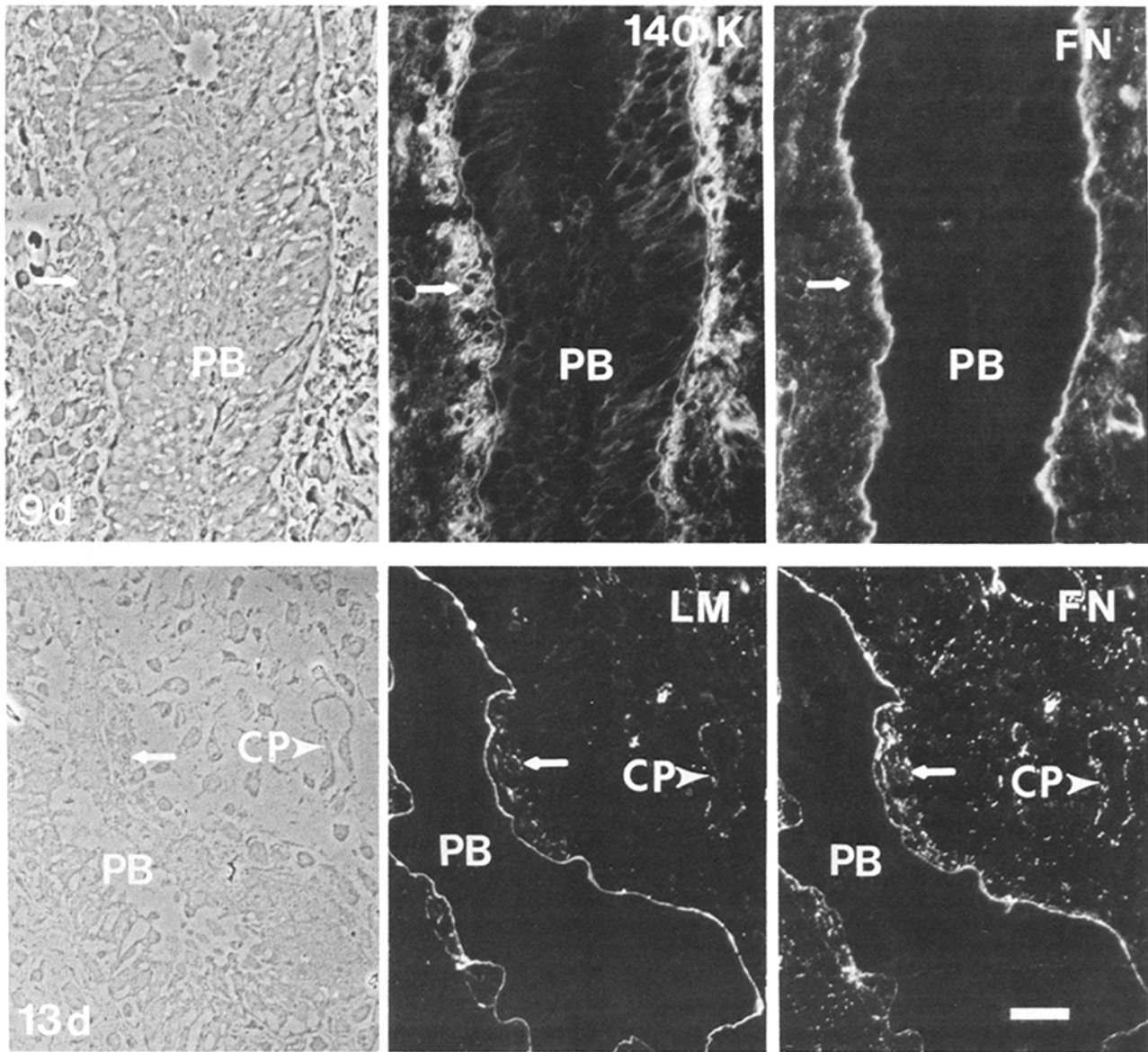
1076
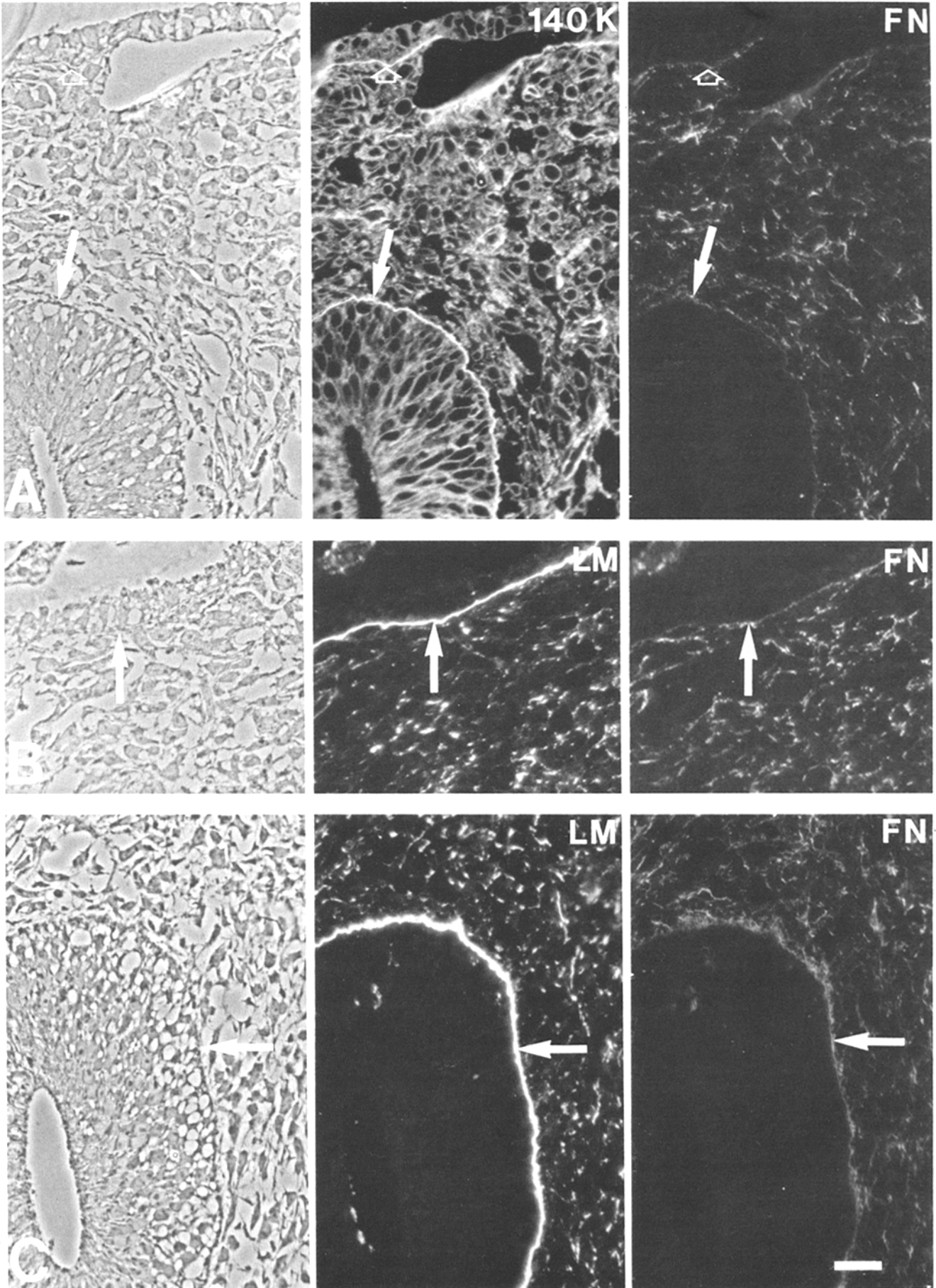
Figure 4. In situ immunofluorescent distribution of 140K complex (*140K*), fibronectin (*FN*), and laminin (*LM*) on FTS of the developing airway in chicken embryonic lungs at mid-glandular period (9 d) and in sections of developing alveoli in embryonic lungs at the early vascular period (13 d). The sections were labeled for 140K complex (monoclonal JG22E) and FN (monospecific rabbit anti-FN), or LM (monospecific guinea pig anti-laminin) and FN, simultaneously. Smooth muscle cells (*arrows*) appear as clusters in the valley between adjacent outpouching parabronchi (*PB*), some are evident in the region of developing alveoli at 13 d. Invading capillaries (*CP*) are also detected in sections of 13-d embryonic lungs. LM is found in the usual basement membrane localization, but FN is labeled throughout the mesenchyme. Bar, 20 μm.

tive number 4.6-fold as development proceeds, from 2.4 × 10^3 cells/mm² (or 17% of total lung cells counted) during the glandular period to 11.0 × 10^3 cells/mm² (or 61% of total lung cells counted) during the alveolar period. Because lung size has increased by a factor of 40, the total increase in number of epithelial cells is ~180-fold. The first capillary endothelial cells appear during the vascular period and they increase in number during the alveolar period. However, as lung size increases, mesenchymal cells become less abundant in the interstitial space, from 83% of total cells counted to 13%, decreasing from 11.7 × 10^3 cells/mm² during the glandular period to 2.7 × 10^3 cells/mm² in the alveolar period. Smooth muscle cells are found at the developing airway regions that occupy 15% of the total sectioned area of

Figure 5. In situ immunofluorescent distribution of 140K complex (*140K*) and fibronectin (*FN*) on FTS of chicken embryonic lungs at the vascular stage, including 13-, 14-, and 16-d egg incubations. (*13, 14,* and *16* d) DIC of lung sections from the embryos at 13, 14, and 16 d of egg incubations. The sections were labeled for 140K complex (monoclonal JG22E) and FN (monospecific rabbit anti-FN), simultaneously. *Arrows,* colocalization of 140K complex and FN at attachment sites between epithelial cells and their basement membranes. *Arrowheads,* sites of 140K complex–FN colocalization on capillary endothelial cells. Note the absence of both 140K complex and FN on the cell surface of blood-borne cells (erythrocytes and leukocytes) in capillaries that are indicated by arrowheads. Bar, 20 μm.
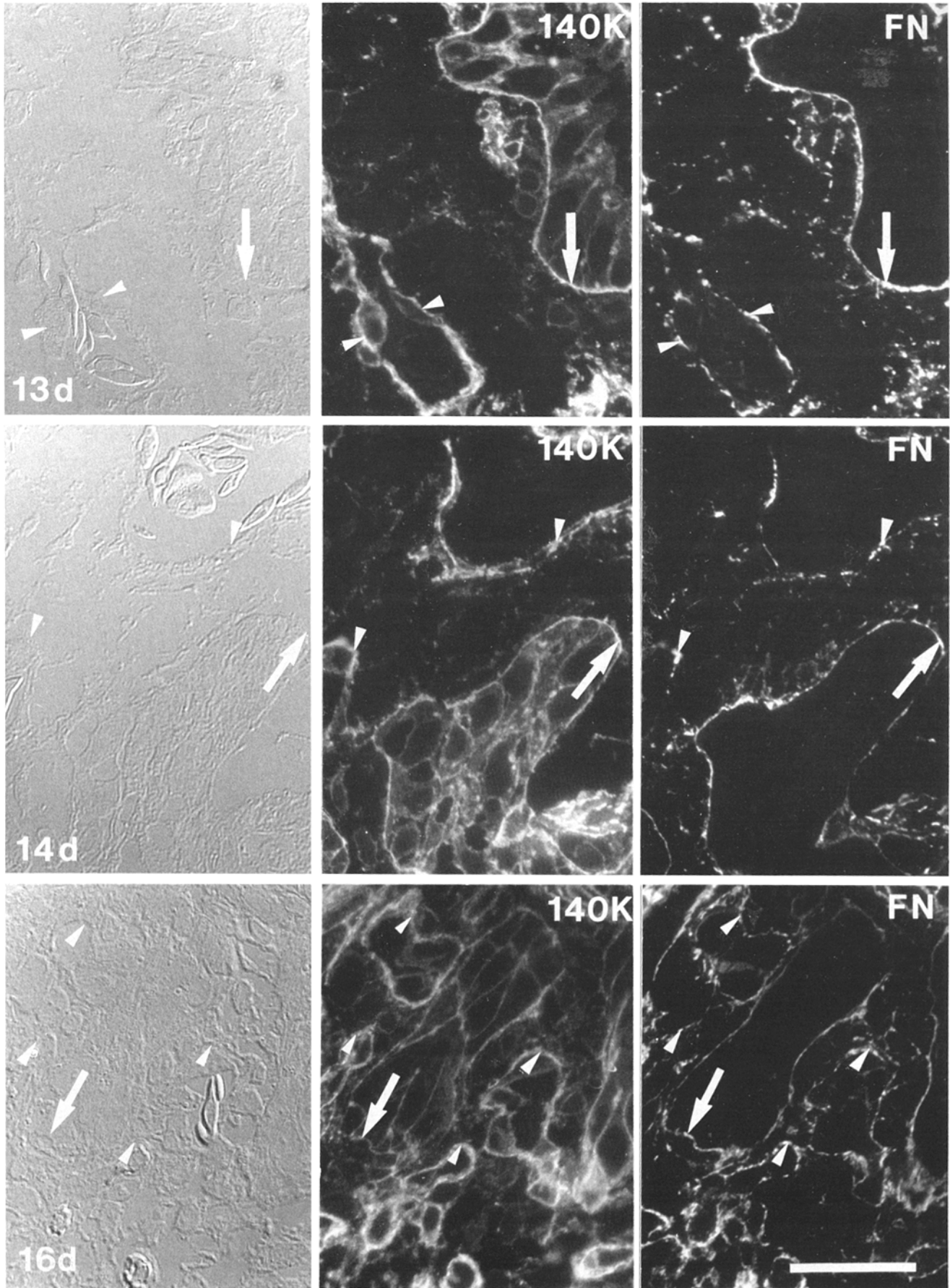
lung at different developmental stages. This percentage remains more or less constant throughout development. After hatching, the alveolar space enlarges at the expense of cell number.

Quantitation of 140K Complex, Fibronectin, and Laminin during the Development of Embryonic Chick Lung by Immunoblot Analysis

The 140K complex, fibronectin, and laminin were detected in embryonic chick lungs by immunoblot analysis. These proteins were previously shown to be present in various tissues and in tissue culture cells (11, 17). Fig. 1 shows Western immunoblots of extracts from lungs at day 18 egg incubation using monospecific rabbit anti–140K complex, fibronectin, and laminin antibodies. Under reducing conditions, anti–140K complex antibodies label a broad band at M_r 125,000–155,000 (probably band 3 since under nonreducing conditions, when all three bands can be resolved, this antibody labels predominantly band 3 with only low levels of bands 1 and 2 detected, see reference 11), anti–laminin antibodies label a sharp band at M_r 220,000 and a narrow band at M_r 440,000 (probably unreduced dimers), and anti–fibronectin antibodies recognize a broad band at M_r 220,000–240,000. To test whether these molecules migrate differently in SDS PAGE when derived from lungs at different developmental stages, we also performed Western immunoblots of lung extracts from embryos at day 5, day 9, and day 13, and from hatched chicks. The immunoblotting patterns of 140K complex, laminin, and fibronectin from lungs at different stages are indistinguishable from each other (not shown) and from those of lungs at day 18 shown in Fig. 1. Thus, 140K complex, as well as laminin, and fibronectin, are present at different stages of lung development in similar molecular forms.

To determine whether 140K complex, fibronectin, and laminin are expressed differentially in embryonic chick lungs, we performed immunodot blot analysis on extracts from embryonic lungs at different stages (Fig. 2). We found that (a) lung fibronectin reached its highest concentration in the late glandular stage to late vascular stage, but was reduced in concentration in the alveolar stage as well as in adult lungs, (b) the 140K complex was also abundant at the alveolar stage and became reduced in the late alveolar stage as well as in adult lungs, and (c) laminin increased in concentration as development proceeded (Fig. 2). The 140K complex, laminin, and fibronectin appear to be expressed in largest quantity by the lung cells that undergo active morphogenetic processes during the vascular period, i.e., epithelial and endothelial cells. Both epithelial and endothelial cells increase in number, while mesenchymal cells rapidly diminish in number during the vascular period of lung development (Table I). Since smooth muscle cells contribute equally high levels of 140K complex during development and are generally restricted to the area around the developing air-

ways (see below), the increased level of 140K complex, laminin, and fibronectin observed during the vascular period might thus functions in the morphogenetic events required during capillary angiogenesis and alveolar wall formation.

140K Complex, Fibronectin, and Laminin Distribution in FTS of Embryonic and Adult Chick Lungs (Figs. 3–12)

We have characterized the distribution of 140K complex, fibronectin, and laminin during lung morphogenesis using double immunofluorescent labeling on 0.5 μm FTS of chick embryos. This methodology provides a high resolution view of lung tissue structure and antigen localization at the cellular level. The 140K complex was found to be present in all types of lung cells during early embryonic stages, as previously demonstrated (3, 19), but was markedly reduced in all of the differentiated lung cell types except smooth muscle cells. We examined in detail the distribution and fate of 140K complex in developing epithelial cells, in angiogenic capillary endothelial cells, during mesenchymal maturation, and during smooth muscle cytodifferentiation, and compared them with those of fibronectin and laminin. Figs. 3–10 represent 140K complex, fibronectin, and laminin stainings of lungs at the glandular, vascular, and alveolar stages, and in adult chicken. The fate of 140K complex, fibronectin, and laminin distribution during the development of alveoli and airways is summarized in Figs. 11 and 12.

Developing Epithelial Cells

When FTS from a lung bud of the chicken embryo at day 5 incubation are reacted with anti–140K complex (JG22E monoclonal antibody) and monospecific anti–fibronectin and anti–laminin polyclonal antibodies, the staining patterns for each are distinctly different (Fig. 3). The 140K complex is localized on both tall, columnar epithelial cells lining the central cavity of the lung bud and short, columnar mesothelial cells covering the lung (Fig. 3, A open arrows; B, arrows). In the epithelium and mesothelium in the early lung bud, both the apical and the basolateral surfaces of the cells exhibit some staining for 140K complex. However, the labeling is greatly enriched at the basal surface where it contacts the underlying basement membrane. Fibronectin staining is punctate although weak on both basement membrane and mesenchyme (Fig. 3, B and C). As expected, laminin stains intensively on basement membranes underlying the epithelia and mesothelia, but most strikingly, laminin is also found in the mesenchyme of the lung bud (Fig. 3, B and C). However, both fibronectin and laminin are absent in the epithelial and mesothelial cell layers (Fig. 3, B and C).

Because the 140K complex was originally identified on chick myoblasts and fibroblasts (11, 25, 38), the specificity of the anti–140K complex monoclonal antibody, JG22E, on lung cells, particularly epithelial cells, was demonstrated by several experiments: (a) monoclonal antibodies JG9 and

Figure 6. In situ immunofluorescent distribution of laminin (*LM*) and fibronectin (*FN*) on FTS of chicken embryonic lungs at the vascular stage. Lung sections from embryos at 13, 14, and 16 d of egg incubations were viewed with DIC. The sections were also immunofluorescently labeled with guinea pig anti–laminin antibody (*LM*) and with rabbit anti–fibronectin antibody (*FN*), simultaneously. *Arrows*, colocalization of LM and FN at epithelial basement membranes. There is a shift of relative LM and FN concentrations on epithelial basement membranes during development. *Arrowheads*, sites of LM–FN colocalization on capillary endothelial cells. LM labeling is absent on the earlier angiogenic cells (13 d). Note the lack of both LM and FN on the cell surface of blood-borne cells (erythrocytes and leukocytes) in capillaries. Bar, 20 μm.
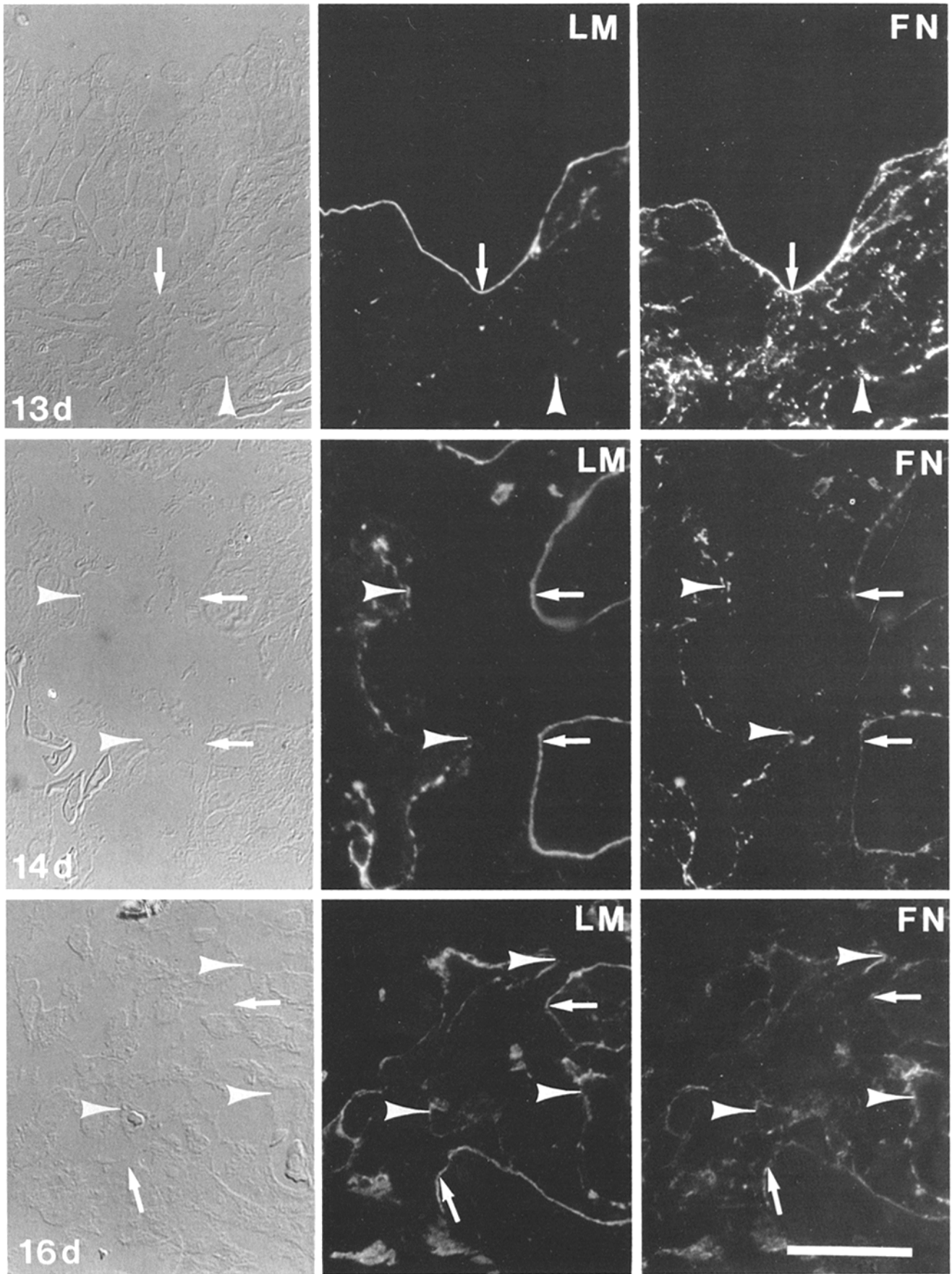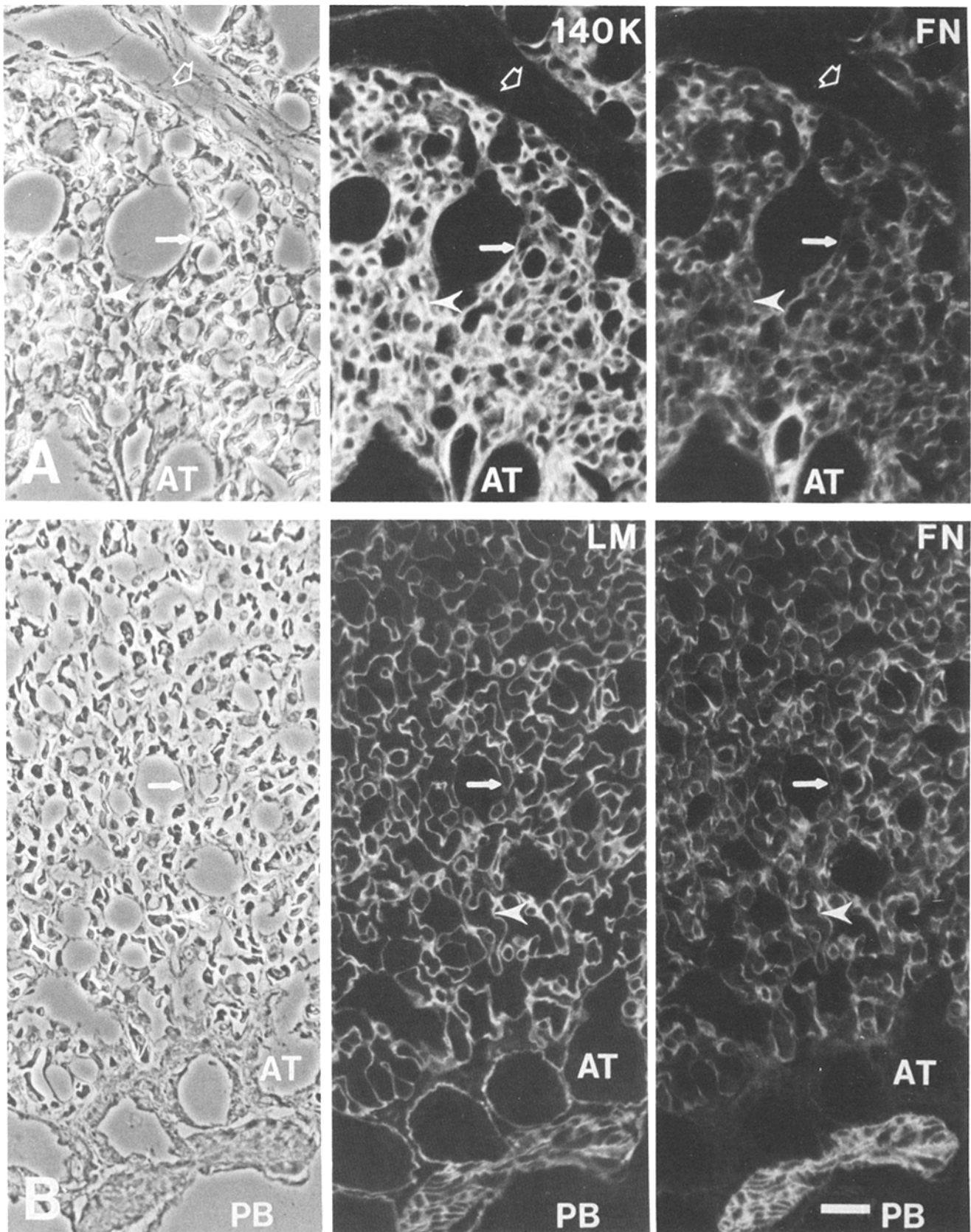
Figure 7. In situ immunofluorescent distribution of 140K complex (*140K*), laminin (*LM*), and fibronectin (*FN*) on FTS of chicken embryonic lungs at the alveolar stage (19 d). (*A*) Phase-contrast view of a section from an embryonic lung at 19 d egg incubation double-labeled with anti–140K complex JG22E monoclonal antibody (140K) and monospecific rabbit anti–fibronectin antibody (*FN*). *Arrows*, developing alveolar sacs. *Arrowheads*, capillaries. The developing alveoli are labeled intensively for 140K complex and FN, whereas the interstitial cells and matrices show very little 140K complex and FN labeling (*open arrows*). (*B*) Phase-contrast view of a lung section adjacent to that

ES186 all showed a staining pattern similar to JG22E monoclonal antibody. JG9 is specific for a determinant of the 140K complex closely related to JG22 (25) and ES186 for a 140K band 3 determinant (Mueller, S., and W.-T. Chen, unpublished result). (b) Monoclonal antibodies produced by a unstable line, JG22, did not show any specific labeling, nor did ET22, a monoclonal antibody directed against an apparent contaminant, band Ia (27). (c) Staining by JG22E monoclonal antibody was completely neutralized by purified fibroblast 140K complex. And, (d) polyclonal anti-140K complex antibodies showed the same staining pattern as JG22E monoclonal antibody, and they competed with JG22E on lung sections when they were added together.

The epithelium lining the central cavity of lung buds first develops into two divisions. By the alveolar period, the epithelium covers a complex network of airways and alveoli. Epithelial cells during the glandular and vascular periods are all stained for the 140K complex, and they undergo a shape change transition as development proceeds: from columnar to cuboidal during the vascular stage (Figs. 5 and 6), and from cuboidal to squamous during the alveolar stage (Figs. 7, 8, and 9). Despite differences in cell shape, most developing alveolar epithelial cells express the 140K complex predominantly on the basolateral surfaces, and preferentially on the basal surface (Figs. 5, 7, 8, and 9). However, developing alveolar epithelia at the glandular stage exhibit some 140K complex staining on both the apical and the basolateral surfaces of the cells (Fig. 3 A). Alveolar cells in adult chicken show significantly lower 140K complex staining (Fig. 10). During the glandular and vascular periods, the epithelium lining the developing airway (parabronchus) displays 140K complex staining only on the basolateral surfaces of the cells (Fig. 4, 9d, and Fig. 5, 13d and 16d). Epithelial cells lining the atria and parabronchi become squamous in shape and complete their differentiation later at the alveolar stage. As they differentiate, their 140K complex labeling becomes punctate and scarce. Lastly, labeling is lost from the basal surface of airway epithelial cells during the alveolar period.

The basal surface of the developing alveolar and airway epithelia is delimited by the laminin-positive basement membranes throughout development. However, fibronectin and laminin staining patterns on basement membranes shift as lungs develop. During the glandular stage, thin layers of basement membranes beneath mesothelium and epithelium stain faintly for fibronectin, but intensely for laminin (Fig. 3, B and C). During the vascular stage, basement membranes transiently acquire higher levels of fibronectin than laminin (Fig. 6, 13d, and Fig. 7 B). Later, throughout the vascular and alveolar periods and after hatching, fibronectin staining is faint and punctate, whereas laminin staining is always continuous and remains intense (Fig. 6, 16d and Fig. 9). The punctate fibronectin staining appears to codistribute with the accumulation of 140K complex on the basal surface of the epithelium contacting the basement membrane (for examples, Fig. 5, 13d and 14d). The alveolar walls of hatched chick exhibit strong 140K complex and laminin labeling and punctate fibronectin staining (Figs. 8 and 9), and later that

of adult lung shows intense laminin staining, weak 140K complex labeling and no fibronectin labeling (Fig. 10 A). In addition, laminin labeling is prominent in basement membranes of airways throughout development, but 140K complex and fibronectin labeling is scarce and punctate on the airways during the alveolar period and at hatching (Figs. 8 and 9) and 140K complex and fibronectin labeling is absent in adult lung airways (Fig. 10 B).

Polarized Distribution of the 140K Complex in Lung Epithelia

To make quantitative comparisons of 140K complex, fibronectin, and laminin distribution on lung FTS, we analyzed their distribution on individual lung cells by photomicroscopic measurements of immunofluorescence, similar to Chuong and Edelman (13). We improved the resolution of measurement by reducing the field window to 3 μm in diameter, small enough to permit measurement of one part of a single cell on the FTS. Because FTS are thinner than individual cells, these measurements reflect the relative amount of antigen per unit cell membrane or structure. During the vascular periods, 140K complex shows the brightest intensities on the basal surface (8 units) of the columnar epithelial cells, eight times brighter than the lateral surfaces (1 unit). The intensity on the basal surface of epithelia at the early glandular stage was 10 units and on the apical and lateral surfaces 2 units. During the alveolar period, epithelia differentiate into airway and alveolar epithelia. When measured on the same section, 140K complex labeling becomes less prominent in the basal surface of alveolar epithelia (3 units), lost in airway epithelia (0 unit), and prominent in smooth muscle (12 units). In adult lungs, the 140K complex is reduced in amount on various cell types, in alveolar epithelia (1 unit), in airway epithelia (0 unit), and in smooth muscle (8 units).

Embryonic Lung Mesenchyme

The mesenchyme of lung buds at the glandular period consists of a large mass of undifferentiated cells that are hexagonal in shape and label intensely for 140K complex, fibronectin, and laminin (Figs. 3 and 11). The mesenchyme undergoes a condensation phase during the vascular period, and the cells become elongated in shape and more sparsely arranged. Although the mesenchyme was labeled for 140K complex, fibronectin, and laminin during the preceding stage, it is weakly labeled for 140K complex and fibronectin, and not detectably labeled for laminin during mesenchymal condensation (Figs. 4, 5, 7, and 11). During the alveolar period, the mesenchyme differentiates into interstitial tissues that are absent from the air–blood barriers and become more sparsely arranged in the thickened alveolar walls. The surface labeling pattern of interstitial cells is similar to mesenchymal cells, i.e., they are only weakly labeled for 140K complex and fibronectin, but not for laminin. In adult lungs, laminin labeling is prominent in the basement membranes of air–blood barriers, punctate 140K complex and fibronectin

shown in A double-labeled for LM and FN. Atria (AT) are identified as large airways branching from the parabronchus (PB). Both developing alveoli and smooth muscle are labeled intensively for LM and FN, whereas the basement membranes lining the atria are stained strongly with LM, but weakly with FN. Bar, 20 μm.
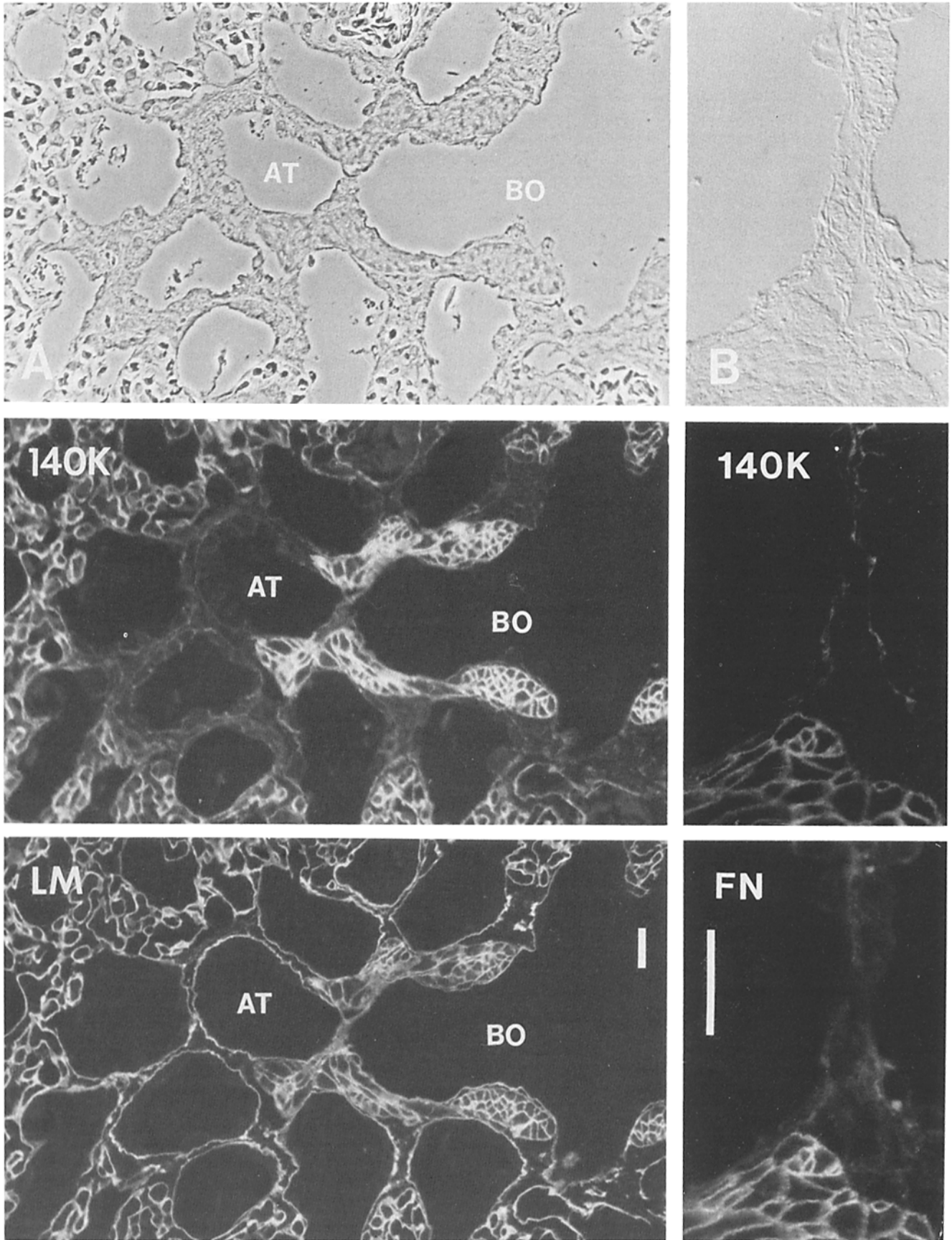
Figure 8. In situ immunofluorescent distribution of 140K complex (*140K*), laminin (*LM*), and fibronectin (*FN*) surrounding the airways of hatched chicken lungs (3 d after hatching). The sections were labeled for 140K complex (monoclonal JG22E) and LM (monospecific rabbit anti-laminin), or 140K complex (monoclonal JG22E) and FN (monospecific rabbit anti-FN), simultaneously. (Column *A*) A lung

labeling is found in the interstitial tissue. Only low levels of 140K complex and no fibronectin labeling is found in the air–blood barriers.

Fibronectin was localized in lung mesenchyme throughout development and it generally codistributes with the 140K complex. However, due to the heterogeneous shape of mesenchymal cells, exact codistribution at the light level is difficult to determine. As expected, laminin is present in the basement membrane underlying epithelia, but in addition, laminin staining is intense in the lung mesenchyme at the early glandular stage (Fig. 3, B and C). Another major basement membrane component, type IV collagen, can also be produced and organized by embryonic mesenchymal cells in explant cultures (8). The amount and distribution of fibronectin appear to shift during development relative to laminin. Laminin is labeled intensely in large patches in mesenchyme at the early glandular stage but fibronectin staining is faint (Fig. 3). During this stage, the punctate laminin and fibronectin label alternates in position in the mesenchyme. After the late glandular stage (Figs. 4, 6, and 7), there is punctate fibronectin labeling, but no detectable laminin.

Angiogenic Capillary Endothelia Cells

Angiogenic invasion of capillaries into embryonic lung mesenchyme occurs during the vascular period (12–16d of egg incubation). Invading capillaries are larger in diameter than differentiated capillaries in adult lungs and are devoid of basement membrane-like structure. The distribution of the 140K complex during capillary angiogenesis and endothelial cell differentiation was studied in detail and compared with that of fibronectin and laminin. During the early vascular period, as capillaries invade the mesenchymal space next to the atria, endothelial cells are relatively large and have a thick cell body (Figs. 5 and 6). Strikingly, the 140K complex is distributed over fibronectin-positive spots at cell–matrix contact sites (Fig. 5, arrowheads). Moreover, there is no detectable laminin labeling at those sites (Fig. 6, 13d, Fig. 11). In the late vascular stage (16d), more continuous fibronectin and laminin labeling surrounds capillaries linking the 140K complex-positive basal portions of endothelial cells (Figs. 5, 6, and 7). Laminin labeling becomes dominant after the late vascular stage (16d). In adult lungs, laminin labeling is prominent in the fused basement membrane of air–blood barriers, but low levels of the 140K complex are present and no fibronectin in these sites (Figs. 10 and 11). In addition, after entry of hematopoietic stem cells into the circulatory system, as seen in the capillaries and other blood vessels in lungs at different developmental stages (Figs. 4–10), there is no detectable labeling for 140K complex, fibronectin, or laminin on these cells.

Smooth Muscle Cytodifferentiation

During the mid-glandular stage, smooth muscle appears as clusters of condensed cells in the loose mesenchyme in val-

leys between adjacent outpouching epithelial tubules. These clusters are first noticed around the developing airways (parabronchi) (Fig. 4, 9d). At this early stage, the 140K complex is distributed evenly on smooth muscle cells and is more abundant on smooth muscle cells (12 units) than on adjacent mesenchymal fibroblasts (3 units) and epithelial cells (8 units). Both fibronectin and laminin are not evident on smooth muscle cells at this stage (see Fig. 4, 9d; laminin not shown). The 140K complex staining becomes punctate, concomitant to the punctate appearance of fibronectin labeling and later of laminin staining, on differentiating smooth muscle cells during the early vascular period (Fig. 4, 13d, and Figs. 5 and 6). During the vascular period, fibronectin labeling intensifies on smooth muscle cells, whereas laminin labeling of smooth muscle is not prominent until the alveolar period (Figs. 4, 13d; 6, 7B, and 8 A). After the vascular period, 140K complex, fibronectin, and laminin remain at relatively high levels on smooth muscle cells throughout the remainder of development. In adult lungs, laminin labeling of smooth muscle remains prominent, while 140K complex and fibronectin label is slightly reduced in intensity.

Discussion

In view of the characteristically different adhesive properties of embryonic cells at various stages of development (45), it is possible that important insights into the mechanisms of morphogenesis and cytodifferentiation will come from a knowledge of how, when, and where cell adhesion molecules, embedded in the plasma membrane, interact with the ECM. To this end, we have analyzed the location and relative amounts of the 140K complex and the ECM molecules fibronectin and laminin during morphogenesis of alveolar walls and cytodifferentiation of mesenchymal and smooth muscle cells, with particular emphasis on the 140K complex. We have found that the level of 140K complex expression is under developmental regulation. The 140K complex is prominently expressed in embryonic lung cell types, including epithelial, endothelial, mesenchymal, and smooth muscle cells, but is markedly reduced in differentiated lung cells except smooth muscle. In addition, the 140K complex was not observed on mature, circulating blood cells, as seen in capillaries and other blood vessels in lungs at different developmental stages (Figs. 4–10). It is unlikely that in differentiated lung cells the JG22E antigenic site of the 140K complex becomes inaccessible or modified in such a way that it cannot be recognized in FTS, because quantitative immunoblotting analysis of the 140K complex using polyclonal rabbit anti–140K complex antibodies agrees with the immunofluorescent results. Thus, it appears that the 140K complex is produced and becomes available for use on most cells in embryonic lungs, but it is lost after differentiation. However, the same 140K complex is probably used in different differentiating lung cells, as 140K complex from lungs of different

---

section viewed with phase-contrast (panel A) and double-label immunofluorescence for 140K complex and LM (bottom panels). Smooth muscle cells are strongly labeled with anti–140K complex antibody (middle panel); alveolar cells are less intensely labeled (left), and the epithelium surrounding the atria (AT) and bronchioles (BO) is not labeled. Basement membranes within the smooth muscle and alveolar regions and those surrounding the atria and bronchioles stain positively for laminin. (Column B) A lung section viewed with DIC (panel B) and double-label immunofluorescence for 140K complex and FN (bottom panels). Smooth muscle cells are labeled with anti–140K complex and anti-FN, but the epithelia and interstitial tissues are stained weakly for 140K complex and FN. Bars, 20 μm.
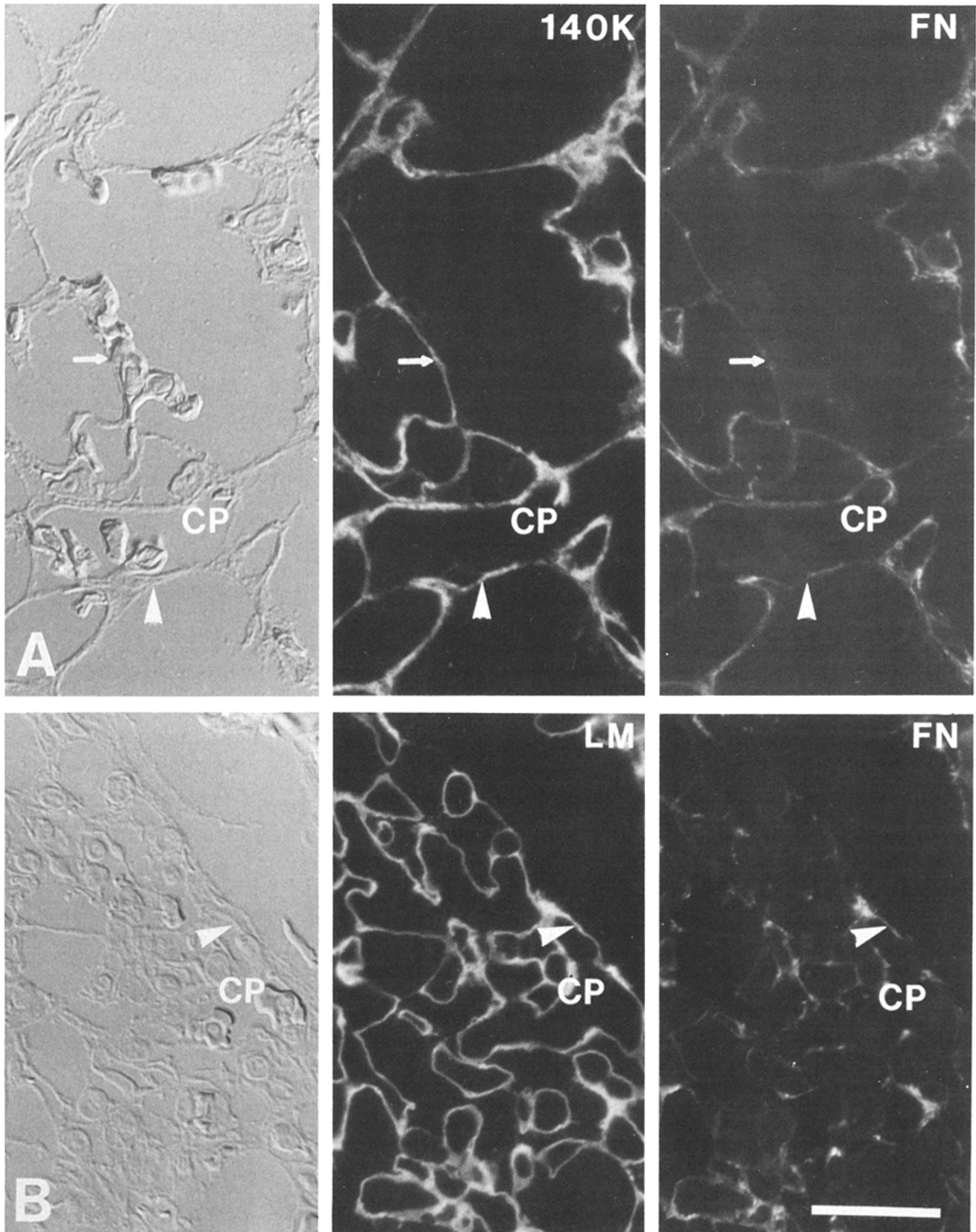
Figure 9. In situ immunofluorescent distribution of 140K complex (*140K*), laminin (*LM*), and fibronectin (*FN*) in alveolar regions of hatched chicken lungs (3 d after hatching) viewed with higher resolution DIC and double-label immunofluorescence. (*A*) DIC view of the expanded alveolar region of a lung section double-labeled with the anti–140K complex JG22E monoclonal antibody (*140K*) and anti-fibronectin (*FN*). *Arrows*, basement membrane of type II pneumocytes and endothelial cells showing colocalization of 140K complex on the basal surface of the type II cells and FN on the basement membrane, while the apical surface of the type II cell is not labeled for 140K complex or FN. *Arrowheads*, basement membrane between type I pneumocytes and capillary (*CP*) endothelial cells showing colocalization of 140K complex and FN. Note that blood-borne cells in the capillary (*CP*) lack cell surface–associated 140K complex and FN. (*B*) DIC view of unexpanded alveolar walls taken from lung sections similar to that in *A*, but labeled with anti-laminin (*LM*) and anti-fibronectin (*FN*). Bar, 20 μm.
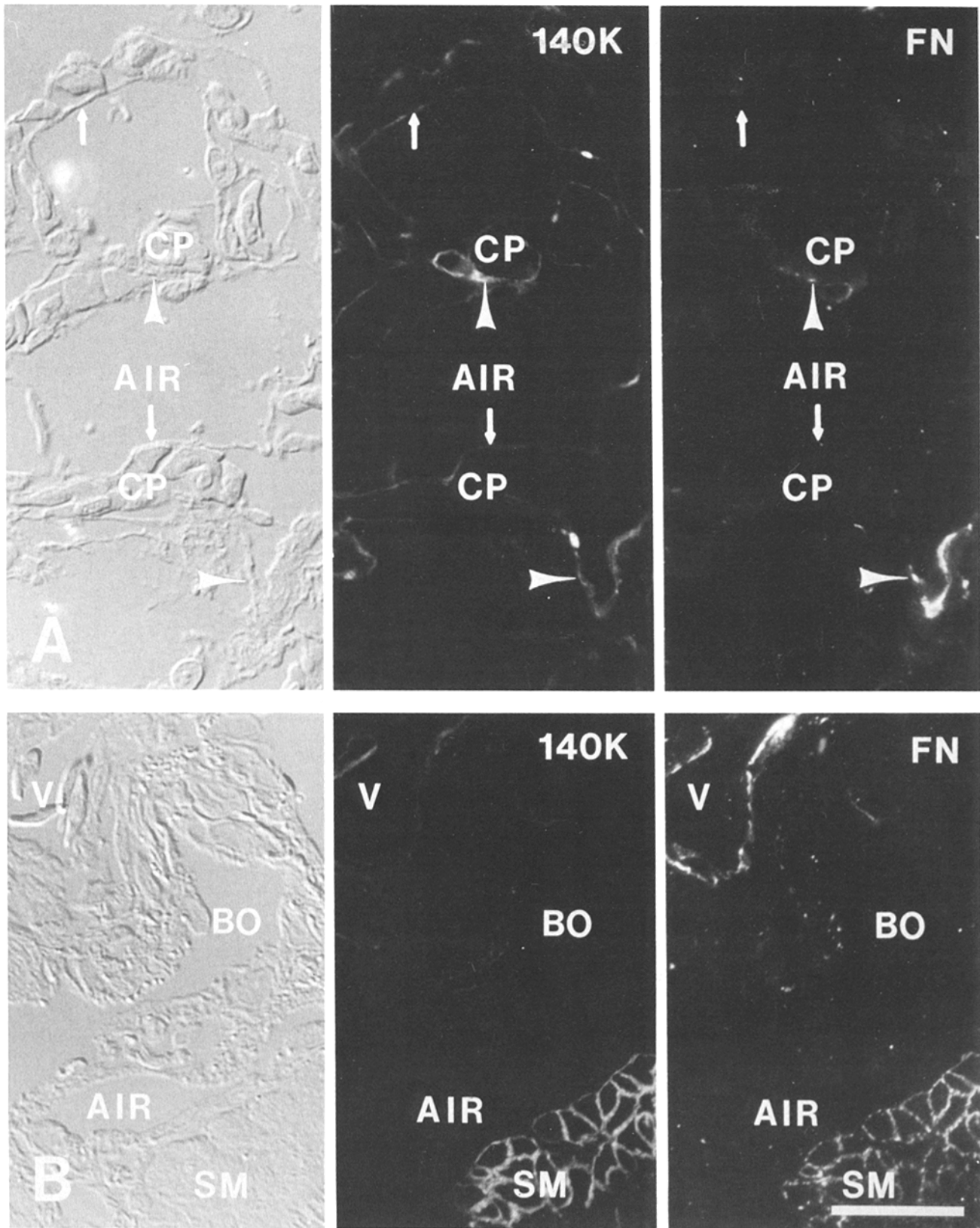
Figure 10. In-situ immunofluorescent distribution of 140K complex (*140K*) and fibronectin (*FN*) in alveolar (*A*) and airway (*B*) regions of adult chicken lungs (3 mo after hatching) viewed with higher resolution DIC and double-label immunofluorescence. (*A*) DIC view of the expanded alveolar region of a lung section double-labeled with the anti–140K complex JG22E monoclonal antibody (*140K*) and anti-fibronectin (*FN*). *Arrows*, basement membrane of pneumocytes and endothelial cells between the air space (*AIR*) and capillary (*CP*), showing weak 140K complex labeling and no FN labeling. *Arrowheads*, interstitial tissue and colocalization of 140K complex and FN. Note that blood-borne cells in the capillary (*CP*) lack cell surface–associated 140K complex and FN. (*B*) DIC view of the airway region taken from lung sections similar to that in *A*. In this section, smooth muscle (*SM*) contains strong 140K complex and FN labeling, veinules (*V*) weak 140K complex and strong FN labeling, whereas epithelia lining the alveoli (*AIR*) and bronchiole (*BO*) lack 140K complex and FN labeling. Bar, 20 μm.
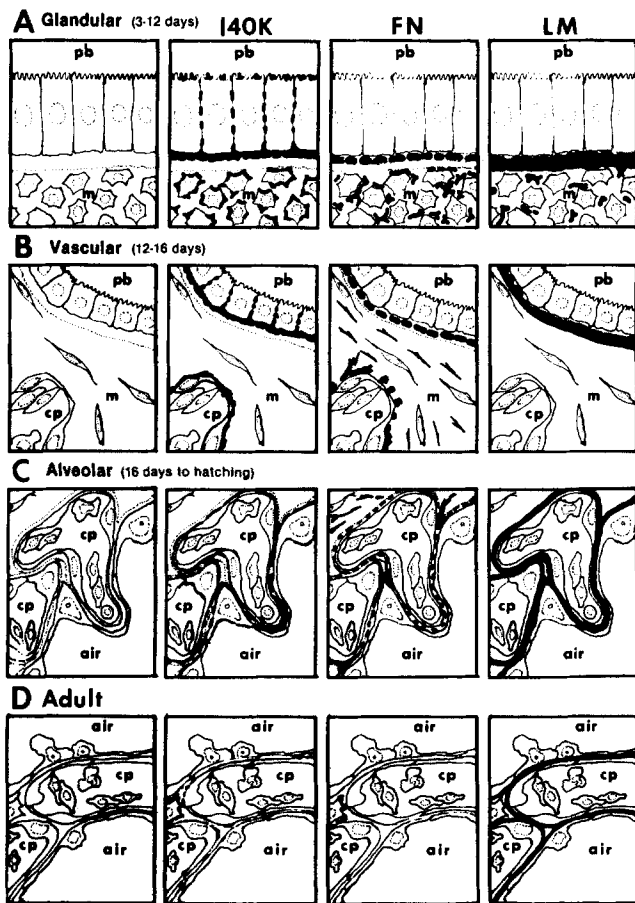
Figure 11. Summary of the distribution of the 140K complex (*140K*), fibronectin (*FN*), and laminin (*LM*) during the development of air–blood barriers in chicken embryonic lungs. The appearance of developing lung during the glandular period (3–12 d) is outlined in *A*, the vascular period (12–16 d) in *B*, the alveolar period (16 d to hatching) in *C*, and the adult in *D*. The first column illustrates the morphology of the developing lung. The last three columns summarize results of double-immunofluorescent labeling experiments. The 140K complex (*140K*), fibronectin (*FN*), or laminin (*LM*) labeling is shown by a dashed or solid line, the thickness indicating the relative intensity of labeling. (*A*) The glandular period. Columnar epithelial cells surrounding the parabronchus (*pb*) show preferential labeling for 140K complex at their basal surfaces adjacent to FN- and LM-positive basement membranes. In the mesenchyme (m), 140K complex, FN, and LM labeling is strong and 140K complex and FN colocalize on mesenchymal cell surfaces. (*B*) The vascular period. In the condensing mesenchyme (m), the cells become elongated in shape and more sparsely arranged. Although the mesenchyme is labeled for 140K complex, FN, and LM during the preceding stage, 140K complex and FN label only weakly, and LM not at all during mesenchymal condensation. The 140K complex and FN colocalize on the cell surface of capillary (cp) endothelia, before LM is detected. (*C*) The alveolar period. Capillary endothelium shares the same basement membrane with alveolar epithelium to form the air–blood barrier. In this basement membrane, LM labeling becomes relatively more prominent, whereas labeling of 140K complex and FN is less prominent. The mesenchyme (m) differentiates into interstitial tissues sparsely arranged within the thickened alveolar walls. These tissues are only weakly labeled for 140K complex and FN, but not for LM. (*D*) The adult. LM labeling is prominent in basement membranes of air–blood barriers, 140K complex labels in a punctate pattern, and FN is not labeled at all. In the interstitial tissue, 140K complex and FN colocalize.
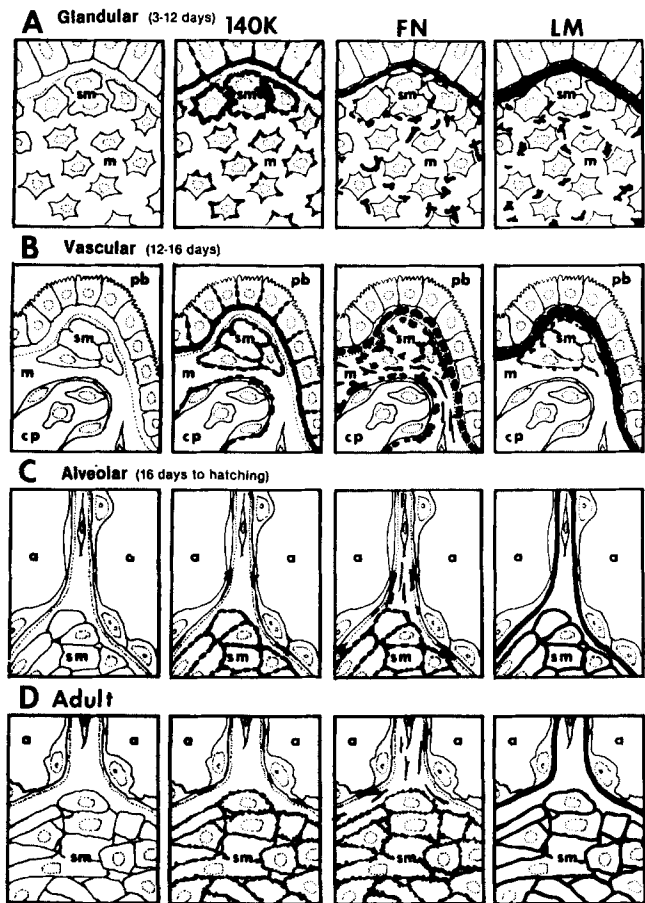
Figure 12. Summary of the distribution of 140K complex (*140K*), fibronectin (*FN*), and laminin (*LM*) during the development of airways in chicken embryonic lungs, with particular emphasis on airway epithelium and smooth muscle differentiation. The appearance of developing lung during the glandular period (3–12 d) is outlined in *A*, the vascular period (12–16 d) in *B*, the alveolar period (16 d to hatching) in *C*, and the adult in *D*. The first column illustrates the morphology of the developing lung. The last three columns summarize results of double-immunofluorescent labeling experiments. The 140K complex (*140K*), fibronectin (*FN*), or laminin (*LM*) labeling is shown by a dashed or solid line, the thickness indicating the relative intensity of labeling. (*A*) The glandular period. A cross section along the valley of outpouching parabronchi. Smooth muscle (sm) first appears as condensations of cells adjacent to the epithelium within the mesenchyme (m) and label more strongly for 140K complex than the surrounding mesenchyme and epithelia. The mesenchyme shows preferential labeling for fibronectin and laminin. (*B*) The vascular period. FN labeling intensifies on smooth muscle cells within valleys formed by the outpouching of the parabronchus (pb), whereas LM labeling of smooth muscle is not prominent until the alveolar stage. (*C*) The alveolar period and *D*, the adult. LM labeling of smooth muscle becomes prominent from the alveolar stage to adult, while 140K complex and FN labeling are reduced slightly in intensity during smooth muscle cytodifferentiation. Epithelial cells lining the atria (a) become squamous in shape and complete their differentiation at the alveolar stage. LM labeling is prominent in the basement membranes of airways, but 140K complex and FN labeling is scarce and punctate.

embryonic ages (when 140K complex is expressed predominantly in different populations of cells) shows the same migration pattern in SDS PAGE.

During lung development, 140K complex expression appears to be independent of fibronectin and laminin, as localized concentrations of 140K complex become evident in the beginning of smooth muscle cytodifferentiation before the accumulation of fibronectin and laminin on the cell surface (Fig. 4). However, the 140K complex on the cell surface of embryonic lung cells is closely associated with extracellular structures rich in fibronectin and laminin. This 140K complex-ECM colocalization was seen in the interactions between all developing lung cells and the ECM or basement membranes. Thus, our results are consistent with the hypothesis that the 140K complex plays an active role in cell-to-matrix adhesion during morphogenesis of alveolar walls and cytodifferentiation of mesenchymal and smooth muscle cells.

In view of the interaction between the 140K complex and fibronectin (1, 28, 40), we believe that fibronectin may play a regulatory role in organizing the 140K complex on the cell surface. In early developing smooth muscle and mesenchymal cells (Figs. 3 A, 4, and 5), 140K complex expressed on the cell surface of embryonic lung cells is redistributed from a uniform to a punctate distribution colocalizing with fibronectin. Furthermore, during the angiogenic invasion of capillaries into lung mesenchyme, 140K complex localizes to sites on the basal surface of endothelial cells in close contact with fibronectin (Fig. 5, 13d). Later, 140K complex and fibronectin colocalize on endothelial cells which subsequently accumulate laminin (Fig. 6). In cultured fibroblasts, the 140K complex is distributed equally between the dorsal and ventral surfaces shortly after plating, but appears to become concentrated on the ventral surface in contact with fibronectin as cell spreading proceeds (12). In motile crest cells, the 140K complex is diffusely organized on the cell surface (19), while in nonmotile cells 140K complex tends to be immobilized in a well-defined area of the cell surface close to fibronectin fibers; the architecture of the fibronectin fibers and their linkage with the cell membrane and with the cytoskeleton appears to be highly ordered and stable (11, 17, 19). Such multivalent fibrillar structures containing fibronectin may organize the 140K complex on the cell surface, providing strong anchorage of cells to the ECM. Additional support for this notion comes from our recent study on Rous sarcoma virus-transformed cells (46). The 140K complex becomes diffusely organized in transformed cells as fibronectin is lost from the cell surface, and reconstitution of fibronectin fibers onto the transformed cell surface causes the reappearance of colocalized 140K complex (46).

Regulation of cell-matrix interactions by cells may be accomplished by cytoskeletal factors acting in concert with pericellular fibronectin assembly via 140K complex. In cultured cells, microfilaments, 140K complex, and fibronectin-containing extracellular fibers colocalize at the cell surface to form linkage complexes (11, 17, 19, 41). In view of the binding interaction between cells and fibronectin, it is reasonable to assume that, to initiate a transmembranous microfilament-140K complex-fibronectin relationship, 140K complex expressed on the cell surface will bind to free fibronectin in the medium. This interaction would then trigger anchorage of microfilaments to the membrane. The resultant transmembrane linkages would lead to increased mobility of the complexes in the plane of the membrane as cytoplasmic mechanochemical forces are generated. As more complexes interact laterally in the membrane, the fibronectin would assemble to form fibers, at the same time stabilizing the complexes and exerting tension on the substrate. Cell detachment from these fibronectin fibers may be favored by low-affinity, reversible binding of cell surface receptors to fibronectin, the involvement of other substrates for cell migration (1, 19) or by fibronectin-degrading proteases (9).

Laminin is a major noncollagenous component of the basement membrane and may regulate the formation of the basement membrane (21, 23, 30, 33) and function in the maintenance of tissues (30, 35). Laminin may have a unique receptor (34, 35, 36) or bind directly to the fibronectin receptor, the 140K complex (28). However, the in vivo functional role of binding between 140K complex and laminin is not known. We have found that there is a temporal and spatial relationship between the appearance of laminin and the disappearance of 140K complex and fibronectin. For example, during epithelial cell differentiation, 140K complex and fibronectin appear first but then diminish as laminin levels increase. Whether laminin plays a possible suppressive role in 140K complex expression during lung cell differentiation requires further examination.

In future experiments, the roles of individual components of the avian 140K complex will be studied by determining the precise localization and temporal sequence of appearance of each during development by using polypeptide-specific monoclonal antibodies. In addition, smooth muscle will be an excellent model for examining the in vivo development of transmembrane actin-140K-ECM complexes and for studying the function of the 140K complex in differentiated tissues. It is possible that the 140K complex interacts with ECM and cytoskeleton in similar ways during motility-related adhesion required for different morphogenetic or differentiated cellular processes, for example, during capillary angiogenesis, airway epithelial branching, and smooth muscle contraction.

References

1. Akiyama, S. K., S. S. Yamada, and K. M. Yamada. 1986. Characterization of a 140-kD avian cell surface antigen as a fibronectin-binding molecule. J. Cell Biol. 102:442–448.
2. Blackburn, W. R. 1974. Hormonal influences in fetal lung development. In Respiratory distress syndrome. Claude Villee, editor. Academic Press, Inc., New York. 271.
3. Bronner-Fraser, M. E. 1985. Alterations in neural crest migration by a monoclonal antibody that affects cell adhesion. J. Cell Biol. 101:610–617.
4. Brown, P., and R. L. Juliano. 1985. Selective inhibition of fibronectin-mediated cell adhesion by monoclonal antibodies to a cell-surface glycoprotein. Science (Wash. DC). 228:1448–1451.
5. Burnette, W. N. 1981. "Western blotting": electrophoretic transfer of proteins from sodium dodecyl sulfate-polyacrylamide gels to unmodified nitrocellulose and radiographic detection with antibody and radiolabeled protein A. Anal. Biochem. 112:195–203.
6. Chapman, A. E. 1984. Characterization of a 140 kd cell surface glycoprotein involved in myoblast adhesion. J. Cell Biochem. 25:109–121.

7. Chen, J.-M., L. Wood, C. Weinstock, and W.-T. Chen. 1985. Distribution of putative 140K ECM receptors in developing chick lung alveoli. *J. Cell Biol.* 101(5, Pt. 2):468a (Abstr.)

8. Chen, J.-M., and C. D. Little. 1985. Cells that emerge from embryonic explants produce fibers of type IV collagen. *J. Cell Biol.* 101:1175–1181.

9. Chen, W.-T., K. Olden, B. A. Bernard, and F.-F. Chu. 1984. Expression of transformation-associated protease(s) that degrade fibronectin at cell contact sites. *J. Cell Biol.* 98:1546–1555.

10. Chen, W.-T., and S. J. Singer. 1982. Immunoelectron microscopic studies on the sites of cell–substratum and cell–cell contacts in cultured fibroblasts. *J. Cell Biol.* 95:205–222.

11. Chen, W.-T., E. Hasegawa, T. Hasegawa, C. Weinstock, and K. M. Yamada. 1985. Development of cell surface linkage complexes in cultured fibroblasts. *J. Cell Biol.* 100:1103–1114.

12. Chen, W.-T., J. M. Greve, D. I. Gottlieb, and S. J. Singer. 1985. The immunocytochemical localization of 140 Kd cell adhesion molecules in cultured chicken fibroblasts, and in chicken smooth muscle and intestinal epithelial tissues. *J. Histochem. Cytochem.* 33:576–586.

13. Chuong, C.-M., and G. M. Edelman. 1985. Expression of cell-adhesion molecules in embryonic induction. I. Morphogenesis of nestling feathers. *J. Cell Biol.* 101:1009–1026.

14. Chuong, C.-M., and G. M. Edelman. 1985. Expression of cell-adhesion molecules in embryonic induction. II. Morphogenesis of adult feathers. *J. Cell Biol.* 101:1027–1043.

15. Compton, S. K. 1979. A study of the morphologic and biochemical differentiation of the developing lung in normal and hypophysectomized chick embryos. Ph.D. Dissertation. Georgetown University, Washington, D.C. 1–186.

16. Compton, S. K., and G. C. Goeringer. 1978. Choline kinase activity in the developing chick lung. *J. Cell Biol.* 79(2, Pt. 2):338a (Abstr.)

17. Damsky, C. H., K. A. Knudsen, D. Bradley, C. A. Buck, and A. F. Horwitz. 1985. Distribution of the cell substratum attachment (CSAT) antigen on myogenic and fibroblastic cells in culture. *J. Cell Biol.* 100:1528–1539.

18. Decker, C., R. Greggs, K. Duggan, J. Stubbs, and A. Horwitz. 1984. Adhesive multiplicity in the interaction of embryonic fibroblasts and myoblasts with extracellular matrices. *J. Cell Biol.* 99:1398–1404.

19. Duband, J.-L., S. Rocher, W.-T. Chen, K. M. Yamada, and J. P. Thiery. 1986. Cell adhesion and migration in the early vertebrate embryo: location and possible role of the putative fibronectin receptor complex. *J. Cell Biol.* 102:160–178.

20. Edelman, G. M. 1983. Cell adhesion molecules. *Science (Wash. DC).* 219:450–457.

21. Ekblom, P. 1981. Formation of basement membranes in the embryonic kidney: an immunohistological study. *J. Cell Biol.* 91:1–10.

22. Gabius, H.-J., W. R. Springer, and S. H. Barondes. 1985. Receptor for the cell binding site of discoidin I. *Cell.* 42:449–456.

23. Garbi, C., and S. H. Wollman. 1982. Basal lamina formation on thyroid epithelia in separated follicles in suspension culture. *J. Cell Biol.* 94:489–492.

24. Gil, J., and A. Martinez-Hernandez. 1984. The connective tissue of the rat lung: electron immunohistochemical studies. *J. Histochem. Cytochem.* 32:230–238.

25. Greve, J. M., and D. I. Gottlieb. 1982. Monoclonal antibodies which alter the morphology of cultured chick myogenic cells. *J. Cell. Biochem.* 18:221–229.

26. Hamburger, V., and H. L. Hamilton. 1951. A series of normal stages in the development of the chick embryo. *J. Morphol.* 88:49–92.

27. Hasegawa, T., E. Hasegawa, W.-T. Chen, and K. M. Yamada. 1985. Characterization of a membrane glycoprotein complex implicated in cell adhesion to fibronectin. *J. Cell. Biochem.* 28:307–318.

28. Horwitz, A., K. Duggan, R. Greggs, C. Decker, and C. Buck. 1985. The CSAT antigen has properties of a receptor for laminin and fibronectin. *J. Cell Biol.* 101:2134–2144.

29. Jahn, J., W. Schiebler, and P. Greengard. 1984. A quantitative dot-immunobinding assay for proteins using nitrocellulose membrane filters. *Proc. Natl. Acad. Sci. USA.* 81:1684–1687.

30. Kleinman, H. K., M. L. McGarvey, J. R. Hassell, and G. R. Martin. 1983. Formation of a supermolecular complex is involved in the reconstitution of basement membrane components. *Biochemistry.* 22:4969–4974.

31. Knudsen, K. A., A. F. Horowitz, and C. A. Buck. 1985. A monoclonal antibody identifies a glycoprotein complex involved in cell-substratum adhesion. *Exp. Cell Res.* 157:218–226.

32. Knudsen, K. A., P. Rao, C. H. Damsky, and C. A. Buck. 1981. Membrane glycoproteins involved in cell-substratum adhesion. *Proc. Natl. Acad. Sci. USA.* 78:6071–6078.

33. Leivo, I., A. Vaheri, R. Timpl, and J. Wartiovaara. 1980. Appearance and distribution of collagens and laminin in the early mouse embryo. *Dev. Biol.* 76:100–114.

34. Lesot, H., U. Kuhl, and K. von der Mark. 1983. Isolation of a laminin-binding protein from muscle cell membranes. *EMBO (Eur. Mol. Biol. Organ.) J.* 2:861–865.

35. Liotta, L. A., C. N. Rao, and S. H. Barsky. 1983. Tumor invasion and the extracellular matrix. *Lab. Invest.* 49:636–649.

36. Malinoff, H. L., and M. S. Wicha. 1983. Isolation of a cell surface receptor protein for laminin from murine fibrosarcoma cells. *J. Cell Biol.* 96:1475–1479.

37. McDonald, J. A. 1986. Roles of fibronectin in lung disease. *In* Fibronectin. D. F. Mosher, editor. Academic Press, Inc., Orlando, Florida. In press.

38. Neff, N. T., C. Lowrey, C. Decker, A. Tovar, C. Damsky, C. Buck, and A. F. Horwitz. 1982. A monoclonal antibody detaches embryonic skeletal muscle from extracellular matrices. *J. Cell Biol.* 95:654–666.

39. Pollerberg, E. G., R. Sadoul, C. Goridis, and M. Schachner. 1985. Selective expression of the 180-kD component of the neural cell adhesion molecule N-CAM during development. *J. Cell Biol.* 101:1921–1929.

40. Pytela, R., M. D. Pierschbacher, and E. Ruoslahti. 1985. Identification and isolation of a 140Kd cell surface glycoprotein with properties expected of a fibronectin receptor. *Cell.* 40:191–198.

41. Rogalski, A. A., and S. J. Singer. 1985. An integral glycoprotein associated with the membrane attachment sites of actin microfilaments. *J. Cell Biol.* 101:785–801.

42. Rosenkrans, W. A. Jr., J. T. Albright, R. E. Hausman, and D. P. Penney. 1983. Ultrastructural immunocytochemical localization of fibronectin in the developing rat lung. *Cell Tissue Res.* 234:165–177.

43. Tadvalkar, G., C. Weinstock, and W.-T. Chen. 1984. Cell–matrix interactions during functional development of chick lung alveoli. *J. Cell Biol.* 99(4, Pt. 2):160a (Abstr.)

44. Torikata, C., B. Villiger, C. Kuhn, and J. A. McDonald. 1985. Ultrastructural distribution of fibronectin in normal and fibrotic human lung. *Lab Invest.* 52:399–408.

45. Trinkaus, J. P. 1984. Cells into organs. The forces that shape the embryo. 2nd ed. Prentice-Hall, Inc., Englewood Cliffs, NJ.

46. Wang, J., C. Weinstock, T. Hasegawa, S. S. Yamada, K. M. Yamada, and W.-T. Chen. 1985. Altered organization of 140K putative ECM receptors in fibroblasts transformed by Rous sarcoma virus or treated with fibronectin cell-binding peptides. *J. Cell Biol.* 101:332a (Abstr.)

47. Yamada, K. M., S. K. Akiyama, T. Hasegawa, E. Hasegawa, M. J. Humphries, D. W. Kennedy, K. Nagata, H. Urushihara, K. Olden, and W.-T. Chen. 1985. Recent advances in research on fibronectin and other cell attachment proteins. *J. Cell. Biochem.* 28:79–97.